

AD-A009 825

CAVITATION BREAKDOWN OF A PUMP OPERATING IN WATER  
HAVING A DILUTE POLYMER CONCENTRATION

M. L. Billet, et al

Pennsylvania State University

Prepared for:

Naval Sea Systems Command

20 March 1975

DISTRIBUTED BY:

**NTIS**

National Technical Information Service  
U. S. DEPARTMENT OF COMMERCE

148100

ADA009825

CAVITATION BREAKDOWN OF A PUMP OPERATING IN WATER  
HAVING A DILUTE POLYMER CONCENTRATION

M. L. Billet and W. S. Gearhart

Technical Memorandum  
File No. TM 75-66  
20 March 1975  
Contract No. N00017-73-C-1418

Copy No. 33

Reproduced by  
NATIONAL TECHNICAL  
INFORMATION SERVICE  
U.S. Department of Commerce  
NIST

The Pennsylvania State University  
Institute for Science and Engineering  
APPLIED RESEARCH LABORATORY  
Post Office Box 30  
State College, PA 16801

NAVY DEPARTMENT

NAVAL SEA SYSTEMS COMMAND

APPROVED FOR PUBLIC RELEASE  
DISTRIBUTION UNLIMITED

UNCLASSIFIED

SECURITY CLASSIFICATION OF THIS PAGE (When Data Entered)

REPORT DOCUMENTATION PAGE		READ INSTRUCTIONS BEFORE COMPLETING FORM
1. REPORT NUMBER TM 75-66	2. GOVT ACCESSION NO.	3. RECIPIENT'S CATALOG NUMBER
4. TITLE (and Subtitle) CAVITATION BREAKDOWN OF A PUMP OPERATING IN WATER HAVING A DILUTE POLYMER CONCENTRATION		5. TYPE OF REPORT & PERIOD COVERED Technical Memorandum
		6. PERFORMING ORG. REPORT NUMBER
7. AUTHOR(s) M. L. Billet and W. S. Gearhart		8. CONTRACT OR GRANT NUMBER(s) N00017-73-C-1418
9. PERFORMING ORGANIZATION NAME AND ADDRESS Applied Research Laboratory P. O. Box 30 State College, PA 16801		10. PROGRAM ELEMENT, PROJECT, TASK AREA & WORK UNIT NUMBERS
11. CONTROLLING OFFICE NAME AND ADDRESS Naval Sea Systems Command Washington, DC 20362		12. REPORT DATE 20 March 1975
		13. NUMBER OF PAGES 44
14. MONITORING AGENCY NAME & ADDRESS (if different from Controlling Office) Naval Ship Research and Development Center Annapolis, MD 21402		15. SECURITY CLASS. (of this report) UNCLASSIFIED
		15a. DECLASSIFICATION DOWNGRADING SCHEDULE
16. DISTRIBUTION STATEMENT (of this Report)  Approved for public release. Distribution unlimited. Per NAVSEA -		
17. DISTRIBUTION STATEMENT (of the abstract entered in Block 20, if different from Report)		
18. SUPPLEMENTARY NOTES		
19. KEY WORDS (Continue on reverse side if necessary and identify by block number)  Axial Flow Pump; Polymer; Cavitation Breakdown		
20. ABSTRACT (Continue on reverse side if necessary and identify by block number)  An experimental program comparing the performance of a single stage axial flow pump operating in both water and a 30 ppm solution of Polycx 301 is discussed in this report. Definitive results demonstrate that higher suction specific speeds at pump breakdown are obtained when pumping a dilute polymer solution. Photographs of pump breakdown are shown for both water and dilute polymer solution.		

DD FORM 1 JAN 73 1473

EDITION OF 1 NOV 65 IS OBSOLETE

PRICES SUBJECT TO CHANGE

SECURITY CLASSIFICATION OF THIS PAGE (When Data Entered)

Subject: Cavitation Breakdown of a Pump Operating in Water  
Having a Dilute Polymer Concentration

References: See Page 11

Abstract: An experimental program comparing the performance of a single stage axial flow pump operating in both water and a 30 ppm solution of Polyox 301 is discussed in this report. Definitive results demonstrate that higher suction specific speeds at pump breakdown are obtained when pumping a dilute polymer solution. Photographs of pump breakdown are shown for both water and dilute polymer solution.

Acknowledgments: This work was supported by NSRDC, Annapolis, Maryland, as a part of their waterjet research and development program.

TABLE OF CONTENTS

	<u>Page</u>
Abstract . . . . .	1
TABLE OF CONTENTS . . . . .	2
LIST OF FIGURES . . . . .	3
INTRODUCTION . . . . .	6
TEST LOOP AND EXPERIMENTAL PROCEDURE . . . . .	6
NONCAVITATING PERFORMANCE . . . . .	8
CAVITATING PERFORMANCE . . . . .	9
SUMMARY AND CONCLUSIONS . . . . .	10
REFERENCES . . . . .	11
FIGURES . . . . .	12

LIST OF FIGURES

<u>Figure No.</u>		<u>Page</u>
1	Schematic of 6-Inch Water Tunnel Pump Test Loop	12
2	Construction and Operating of Friction Tube	13
3	Schematic of Instrumentation	14
4	Head Coefficient Versus Flow Coefficient for Axial Pump	15
5	Pump Efficiency Curve	16
6	Pump Loading for Flow Coefficient of 0.203, 2747 RPM, and in Water	17
7	Pump Loading for Flow Coefficient of 0.195, 2750 RPM, and in 30 ppm Polymer Solution	18
8	Pump Loading for Flow Coefficient of 0.279, 2740 RPM, and in Water	19
9	Pump Loading for Flow Coefficient of 0.271, 2750 RPM, and in 30 ppm Polymer Solution	20
10	Pump Loading for Flow Coefficient of 0.305, 2745 RPM, and in Water	21
11	Pump Loading for Flow Coefficient of 0.305, 2753 RPM, and in 30 ppm Polymer Solution	22
12	Pump Loading for Flow Coefficient of 0.280, 1667 RPM, and in Water	23
13	Pump Loading for Flow Coefficient of 0.276, 1660 RPM, and in 30 ppm Polymer Solution	24
14	Pump Performance as a Function of Torque and Suction Specific Speed for a Flow Coefficient of 0.280 in Water	25
15	Pump Performance as a Function of Torque and Suction Specific Speed Operating in Water and Polymer Solution at a Flow Coefficient of 0.280 at 2750 RPM	26

LIST OF FIGURES (Cont'd)

<u>Figure No.</u>		<u>Page</u>
16	Pump Performance as a Function of Torque and Suction Specific Speed Operating in Water and Polymer Solution at a Flow Coefficient of 0.280 at 1667 RPM	27
17	Summary of Pump Performance at a Flow Coefficient of 0.280 and both 2752 and 1662 RPM	28
18	Pump Performance as a Function of Torque and Head Operating in Water and Polymer Solution at a Flow Coefficient of 0.280 at 1667 RPM	29
19	Pump Performance as a Function of Torque and Head Operating in Water and Polymer Solution at a Flow Coefficient of 0.280 at 2750 RPM	30
20	Pump Performance as a Function of Torque and Suction Specific Speed Operating in Water and Polymer Solution at a Flow Coefficient of 0.195 at 2748 RPM	31
21	Pump Performance as a Function of Torque and Head Operating in Water and Polymer Solution at a Flow Coefficient of 0.195 at 2748 RPM	32
22	Pump Performance as a Function of Torque and Suction Specific Speed Operating in Water and Polymer Solution at a Flow Coefficient of 0.305 at 2753 RPM	33
23	Pump Performance as a Function of Torque and Head Operating in Water and Polymer Solution at a Flow Coefficient of 0.305 at 2753 RPM	34
24	Summary of Polymer Influence on Pump Performance	35

LIST OF FIGURES (Cont'd)

<u>Figure No.</u>		<u>Page</u>
25	Index for Photographs of Pump Operating in Water and Polymer Solution at a Flow Coefficient of 0.280 at 2750 RPM	36
26	Photographs of Cavitating Pump Operating in Water and Polymer Solution	37



## INTRODUCTION

It has been known for some time that drag-reducing polymers inhibit the inception of cavitation for some flow situations. Early experimental investigations conducted by Ellis [1] showed that the polymer content of the water has a large effect on both cavitation inception and its appearance on a hemispherical nosed cylindrical body. Photographs of developed cavitation on such bodies illustrate a reduction in cavity size for the same cavitation index when polymers of dilute concentration are present in water. There also seems to be a noticeable difference in the appearance of developed cavities [2,3] in the polymer solution as compared to those formed at the same cavitation index in pure water.

More recent experimental investigations [4,5] extend the results of Ellis for hemispherical nose shapes in a polymer solution. Also, work is being done on the influence of polymer solutions on jet cavitation [6] and on the bubble dynamics [7,8]. A survey of the state-of-the-art on effects of polymer additives on inception is given by Acosta and Parkin [4].

This evidence on the inhibition of cavitation suggested that the presence of polymers in water could suppress the cavity growth of cavitation in the blade passage of a pump. If so, the pump could operate at lower net positive suction heads and thereby attain higher suction specific speeds before performance breakdown.

A series of experimental tests on a single stage axial flow pump were undertaken to provide definitive information if higher suction specific speeds would be obtained when pumping a dilute polymer solution.

The results of the performance of a single stage axial flow pump operating in both water and a dilute polymer solution are discussed in this report. The interest in determining the performance of a pump operating in a dilute polymer solution arises with regards to application on high speed hydrofoil craft. The intent being that polymer injection would occur at the inlet of the waterjet intake system during hump or take-off conditions. The associated increases in pump shaft speed and pump inlet velocity as well as changes in pump size and weight could make such an arrangement feasible.

## TEST LOOP AND EXPERIMENTAL PROCEDURE

The test loop which was designed for the experimental evaluation of an axial flow pump operating in water and a dilute polymer solution is shown schematically in Figure 1. It consists of a closed loop tunnel having a 6-inch diameter plexiglass test section. The main drive pump of the tunnel is a double suction centrifugal pump powered by a variable speed drive system. Tunnel velocity can be varied by controlling the shaft speed of this pump. The pressure control system is independent of tunnel velocity permitting a range of cavitation performance to be obtained at a given velocity. The air content level

was controlled by air collection domes located at the top of the tunnel. These were designed to collect and discharge the free gas which was removed from the water with a vacuum. In this manner all tests were run with the air content of the water at a relatively constant value of 8 ppm.

The single stage axial flow pump was mounted in the test section of the water tunnel and driven by a variable speed 70 HP electric motor located outside the tunnel. The shaft from the motor to the pump rotor was strain gauged to measure shaft torque and a rpm counter on the motor indicated shaft speed. The total pressure upstream of the rotor was measured in the settling section forward of the pump. The tunnel velocity in the test section was checked by a previous calibration which consisted of photographing the passage of air bubbles through the test section over a given time interval. By this means, test section velocity was obtained and correlated with the pressure drop across the entrance nozzle to the test section. This calibration was accomplished with pure water and when a dilute polymer solution filled the tunnel.

The total head downstream of the pump was measured by means of a wedge-type yaw probe traverse located just aft of the stator blade row. The traverse provided local velocity and total pressure at any radius and thereby permitted a mass averaged head rise across the pump stage to be calculated. This energy traverse was performed when both water and polymer was being pumped. It has been shown that when polymers are used that some error is normally associated with total pressure readings [9] and the data presented for polymer solutions should be analyzed with this in mind.

The axial flow pump stage used was originally designed as a propulsor on the aft of a body of revolution. For this reason it was originally designed to operate in the boundary layer coming from the hull of the body. For its original application, the axial velocity component near the blade hub sections is less than that experienced by the blade tips; however, in its operation in the test loop the axial velocity was essentially constant across the blade span. This deviation in the inlet velocity profile from that which the pump stage was originally designed for, results in the blade sections operating at an off-design condition from tip to root and subsequently the pump stage gave a relatively low stage efficiency when tested in the tunnel test loop.

The polymer used in the experiment was Polyox WSR-301 at a concentration of 30 pounds of polymer per million pounds of water (ppm) in the 6-inch water tunnel. This polymer solution was prepared by uniformly aspirating the dry polymer with tap water. The solution was kept under a vacuum aged in a container before being injected into the tunnel to form a polymer ocean.

Therefore, the concentration of the polymer was fixed; however, the changing polymer state was monitored by a friction tube as shown in Figure 2. The results of this device can be related to the molecular weight distribution and an equivalent fresh polymer concentration as discussed by Berman [10]. However, the usefulness of this device is limited because of the limitation on tube Reynolds number, and on the shear rate as measured by the device.

Preliminary results showed that the friction tube indicated that the polymer solution in the tunnel was essentially water after ten minutes of tunnel operation. The usefulness of the friction tube was restricted to the assurance that the initial polymer solution had maximum drag reduction effectiveness at all tube Reynolds numbers.

A schematic of the instrumentation used for evaluating the performance of the axial flow pump stage is shown in Figure 3. The data was visually observed, recorded and subsequently reduced on an IBM 1130 computer. It was originally thought that the installation of the axial flow pump stage in the 6-inch test section in series with the main drive pump of the tunnel would permit a relatively wide range of flow coefficients. This was to be accomplished by holding the shaft speed of the axial flow pump in the test section constant and varying the shaft speed of the main drive pump of the tunnel. It was found, however, that this was not possible since the power available to the main drive pump was not sufficient. It was therefore necessary to install orifice plates of various diameters in the vertical legs of the tunnel and by this means vary the pressure drop in the tunnel and obtain a range of flow coefficients. Three different orifice plates were used and by this means a limited number of flow coefficients could be obtained when the pump was subject to low inlet pressures and operated with profuse cavitation.

#### NONCAVITATING PERFORMANCE

The overall noncavitating performance is shown in Figure 4 as head rise coefficient versus flow coefficient. A similar plot of stage efficiency versus flow coefficient is shown in Figure 5. The efficiency curve indicates that peak efficiency for this axial stage is near 0.26 and indicates a peak efficiency of 0.62. As previously explained, this pump stage had originally been designed for use on the aft of an axisymmetric body as a wake adapted propulsor. The blade sections were therefore designed to accommodate an axial inflow that had considerable variation in velocity and energy along the span of the blade from hub to tip. As the rotor and stator was mounted in the test section of the water tunnel, the velocity and energy at rotor inlet was constant along the blade span. The blade sections are therefore operating at an off-design condition and results in the low value of stage efficiency that was recorded. The total head rise across the stage was measured by means of a wedge probe traverse. The probe had a total pressure port which had a diameter of approximately 0.040". The accuracy of the total pressure measurements in polymer solutions is dependent on port diameter, velocity, and polymer concentration [9]. For this reason, the spanwise measurements of total head rise as a function of radial distance from tunnel centerline shown in Figures 7, 9, 11, and 13 should be viewed with some caution since a polymer solution of 30 ppm was being pumped and the estimated error is five percent. Similar plots using plain water in the tunnel are shown by Figures 6, 8, 10, and 12.

An attempt was made to obtain data at the same flow coefficient when water and polymer was used. However, some slight variation did occur in flow coefficient, the maximum being about 3 percent. Essentially, the same spanwise distribution of head rise occurred when using either water or polymer at the same flow coefficient. The measured efficiency was

consistently lower when polymer was pumped but this could be attributed to the above described inaccuracies associated with total head readings in polymers.

#### CAVITATING PERFORMANCE

The procedure for obtaining the cavitating performance of the axial flow pump stage differed from that when noncavitating performance was obtained. It was found that as the total pressure at pump inlet was decreased and cavitation became progressively more profuse in the passages of the pump that the flow rate began to decrease. It was necessary to constantly adjust the shaft speed of the main tunnel pump to maintain the tunnel velocity at a constant value and maintain a constant flow coefficient through the entire range of cavitation from inception to performance breakdown.

Cavitation tests were performed on the axial flow pump when the tunnel was filled with water and alternately when filled with a polymer solution having a concentration of 30 ppm of Polyox. The flow of the polymer around the tunnel and through the pumps tended to degrade it rapidly with time; however, for times up to 15 minutes, its degraded state was still relatively effective on cavitation performance. As previously discussed, the measurement of head rise through the pump stage is difficult to obtain with polymers due to the inaccuracy of total head measurements. It was decided that shaft torque would be monitored as the total head at pump inlet was varied. This torque was nondimensionalized by the shaft torque that existed at noncavitating conditions.

Three flow coefficients were run to obtain the cavitating performance data. These were all the flow coefficients that could be obtained with the orifice configurations available and the power range of the main tunnel pump.

At a flow coefficient of 0.280, which is near to the peak efficiency of the pump stage, a plot is shown in Figure 14 of the nondimensionalized shaft torque versus suction specific speed when pure water was pumped. Figure 15 presents a similar plot when a 30 ppm polymer solution is pumped. Superimposed on this figure is the water data and it illustrates a significant change in the suction specific speed at which performance breakdown occurs when a polymer solution is pumped. Approximately a 25 percent increase in suction specific speed is achieved before breakdown occurs when polymer is present.

The effect of the polymer solution on performance may be partially related to the shear rate of the polymer at the blade surface. The importance of shear rate was evident by reducing the pump shaft speed from 2742 to 1667 rpm while maintaining the same flow coefficient. The effect of this decrease in shaft speed on cavitation performance is illustrated in Figures 16 and 17. As reported for hemispherical nosed bodies [5], the results show a decreasing effect of the polymer solution on cavitation performance as the shear rate decreases.

Whereas the decrease in shaft torque as a function of suction specific speed is rather gradual, the pump performance in a polymer solution is much more pronounced if plotted against the nondimensionalized total head at pump inlet. The results of both 2750 and 1667 rpm shaft speed are shown in Figures 13 and 19 for a flow coefficient of 0.280.

Similar plots of shaft torque versus suction specific speed and total head at pump inlet for flow coefficients of 0.195 and 0.305 are shown by Figures 20 thru 23. The improvement in suction specific speed before performance breakdown occurs is evident from these curves; however, the increase is not as great for off-design performance as that for a flow coefficient of 0.28. A plot in Figure 24 indicates the change in cavitation performance at three flow coefficients when water and polymer are used.

Of significance in Figure 24 is the reduced effect of polymer at flow coefficients other than that near the design condition or that near where peak efficiency occurs. This effect may result from the blades operating at such an off-design flow incidence that the flow about the blade leading edge is of a nature that the polymers can not act to suppress the degree of cavitation.

The details of the cavitation patterns on the rotor with and without polymers is shown by the photographs in Figures 26 near design operating conditions. Figure 25 is a key to these photographs in that the numbers on the photographs correspond to the numbers marked on Figure 25 and identify the suction specific speed at which the pictures were taken.

Although some of the pictures do not show reduction of one type of cavitation versus others, some definitive conclusions can be made. Firstly, the structure of the cavitation bubbles appears smaller in water than in the similar polymer cases. This could be related to the drastically lowered surface tension in a polymer solution. Secondly, the quantity of cavitation on the blades and in the passage is reduced in the polymer solution for equivalent amounts of reduced torque.

#### SUMMARY AND CONCLUSIONS

The tests indicate that a dilute polymer solution increases the suction specific speed at which cavitation effects the overall performance of an axial flow pump. The improvement in resistance to cavitation breakdown is more pronounced near the design flow coefficient than at off-design conditions.

The added resistance to cavitation performance breakdown was found to be dependent on pump shaft speed and this result is not inconsistent with past results on the cavitation suppression of polymer solutions. This effect has been reported in Reference [4] with regard to incipient cavitation and indicates that some consideration with respect to scale must be exercised before directing this technique to a particular application.

REFERENCES

1. Ellis, A. T., "Some Effects of Macromolecules on Cavitation Inception and Noise," Calif. Inst. of Tech. Report under Contract NC0530-12164, 1967.
2. Hoyt, J. W., "Effects of High-Polymer Solutions on a Cavitating Body," Proc. of 11th Int'l Towing Tank Conference, Tokyo, 1966.
3. Brennen, C., "Some Cavitation Experiments with Dilute Polymer Solutions," J. Fluid Mech. 44, 1970.
4. Acosta, A. J. and Parkin, B. R., "Cavitation Inception--State of the Art," Proc. of 17th American Towing Tank Conference, Pasadena, Calif., 1974. See also J. of Ship Research, 1975, in press.
5. Holl, J. W., Arndt, R. E. A., Billet, M. L., and Baker, C. B., "Cavitation Research at the Garfield Thomas Water Tunnel," Proc. of the Inst. of Mech. Eng. Cavitation Conference, Heriot-Watt Univ., Edinburgh, 1974.
6. Hoyt, J. W., "Jet Cavitation in Polymer Solutions," ASME Cavitation and Polyphase Flow Forum, 1973.
7. Ellis, A. T. and Ting, R. Y., "Bubble Dynamics in Drag Reducing Polymer Solutions," Univ. of Calif., San Diego, Dept. of Aero. and Mech. Eng., Final Report under NUC Contract N66001-70-C-0237, 1960.
8. Ellis, A. T. (et al.), "Cavitation Suppression and Stress Effects in High-Speed Flows of Water and Dilute Macromolecular Additives," J. Basic Eng., Trans. ASME, Series D, 92, 1970.
9. Berman, N. S., Gurney, G. B., and George, W. K., "On Pitot Tube Errors in Dilute Polymer Solutions," Physics of Fluids Letters, Vol. 16, No. 9, Sept. 1973.
10. Berman, N. S., "The Interpretation of Polymer Data," ARL TM #73-53, April 6, 1973.

20 March 1975  
MLB:WSG:1hm

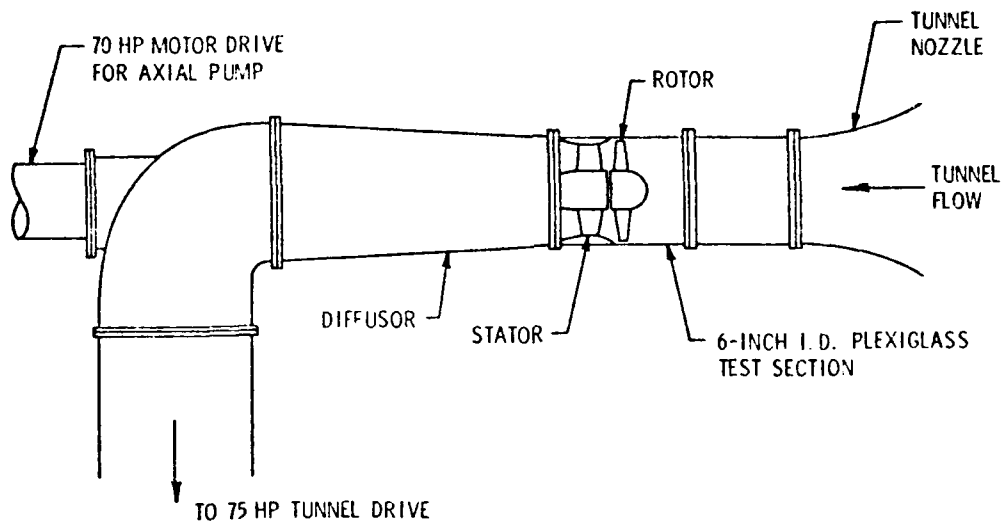
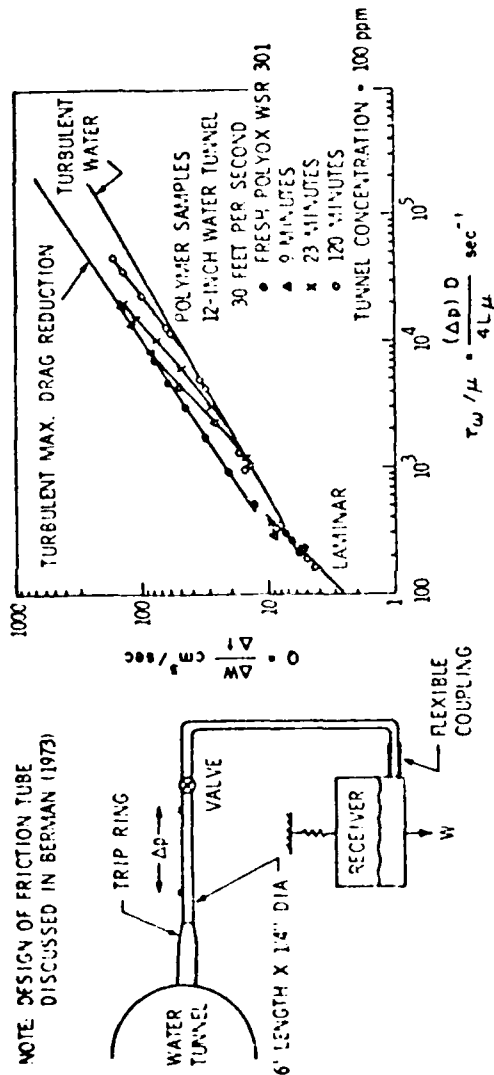


Figure 1: Schematic of 6-inch Water Tunnel Pump Test Loop

20 March 1975  
MLB:WSG:1hm



#### OPERATING PROCEDURE

1. PRESSURE DIFFERENCE IS CREATED BETWEEN TUNNEL AND EMPTY RECEIVER.
2. FLOW IS INITIATED BY OPENING VALVE; PIPE PRESSURE DROP ( $\Delta P$ ) AND RECEIVER WEIGHT ( $W$ ) ARE CONTINUOUSLY RECORDED. RUN IS TERMINATED WHEN RECEIVER PRESSURE EQUALS TUNNEL PRESSURE (TYPICAL RUN TIME ~ 40 SECONDS).
3. WALL SHEAR STRESS AND MASS FLOW RATE ARE CALCULATED AND PLOTTED AUTOMATICALLY.
4. RECYCLE TIME ~ 1 MINUTE.

Figure 2: Construction and Operating of Friction Tube



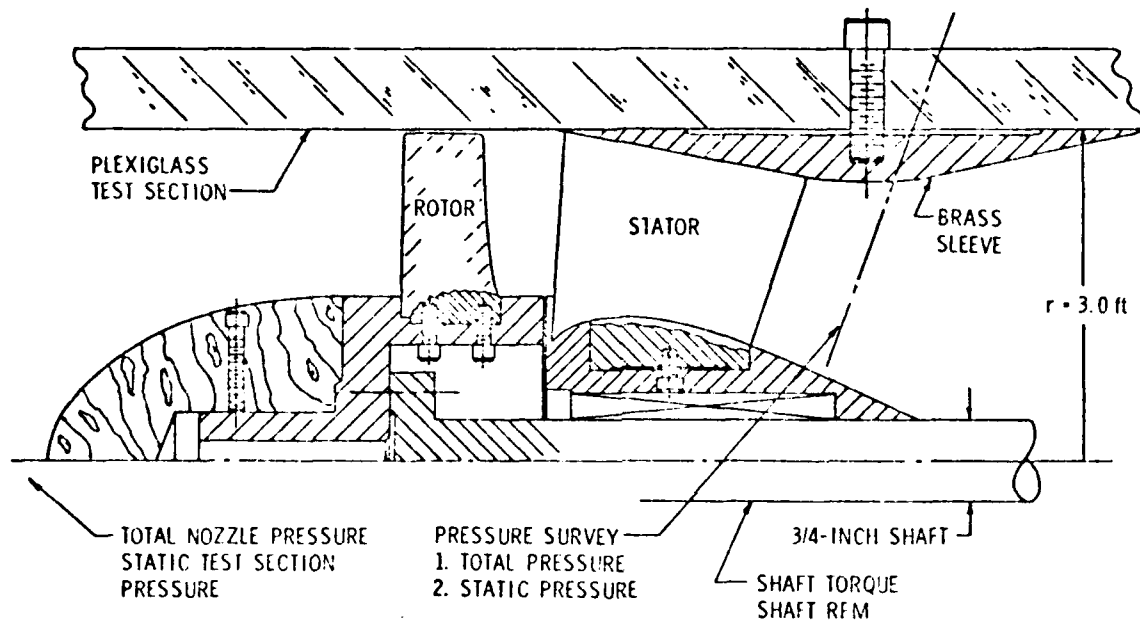


Figure 3: Schematic of Instrumentation

20 March 1975  
MLB:WSG:1hm

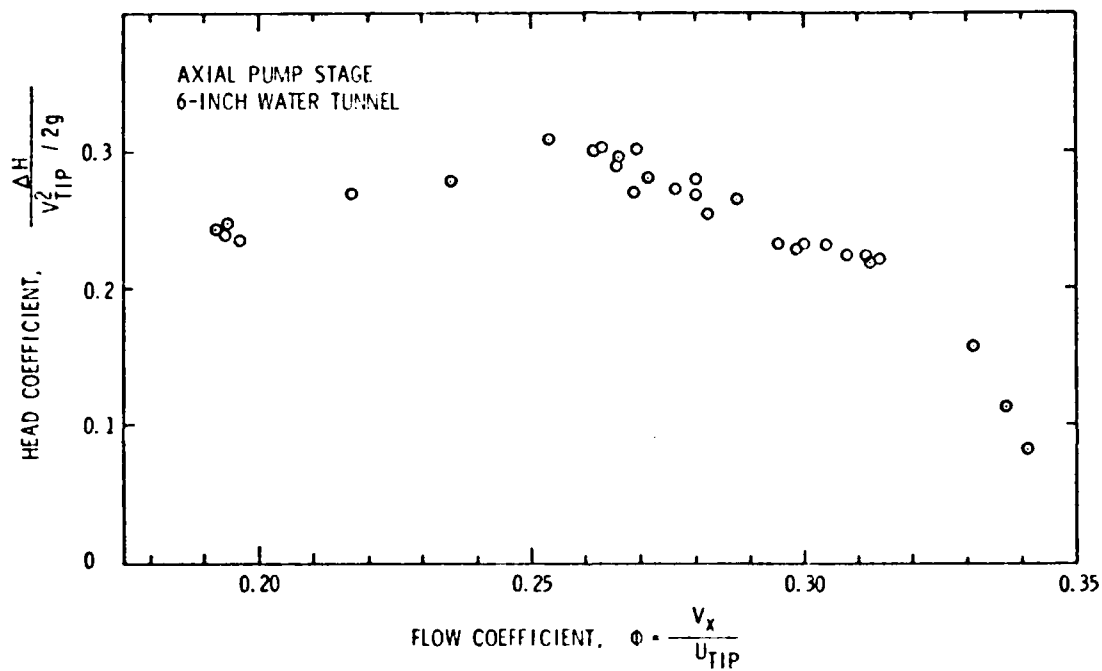


Figure 4: Head Coefficient Versus Flow Coefficient for Axial Pump

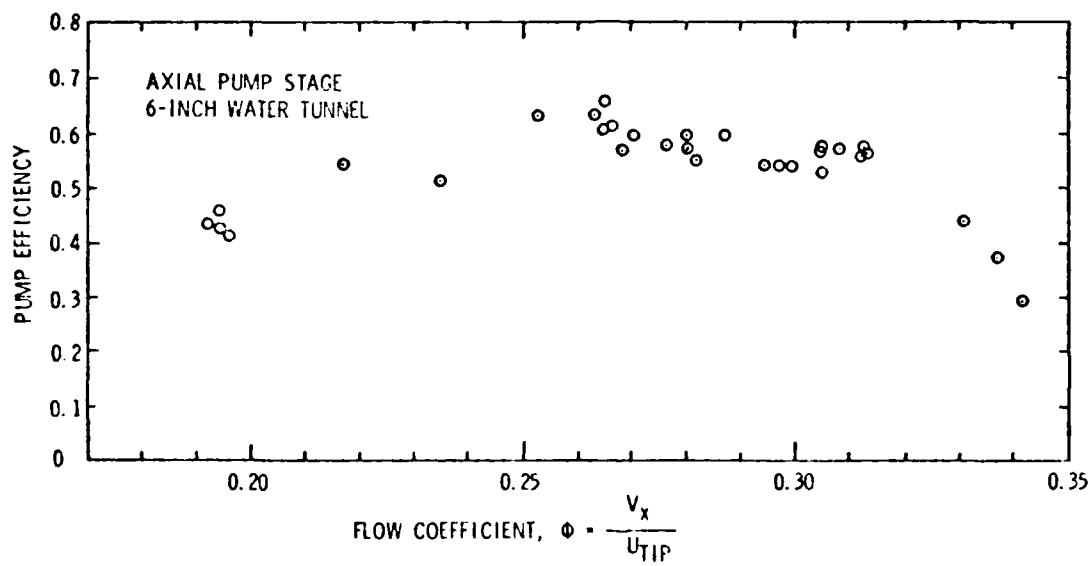


Figure 5: Pump Efficiency Curve

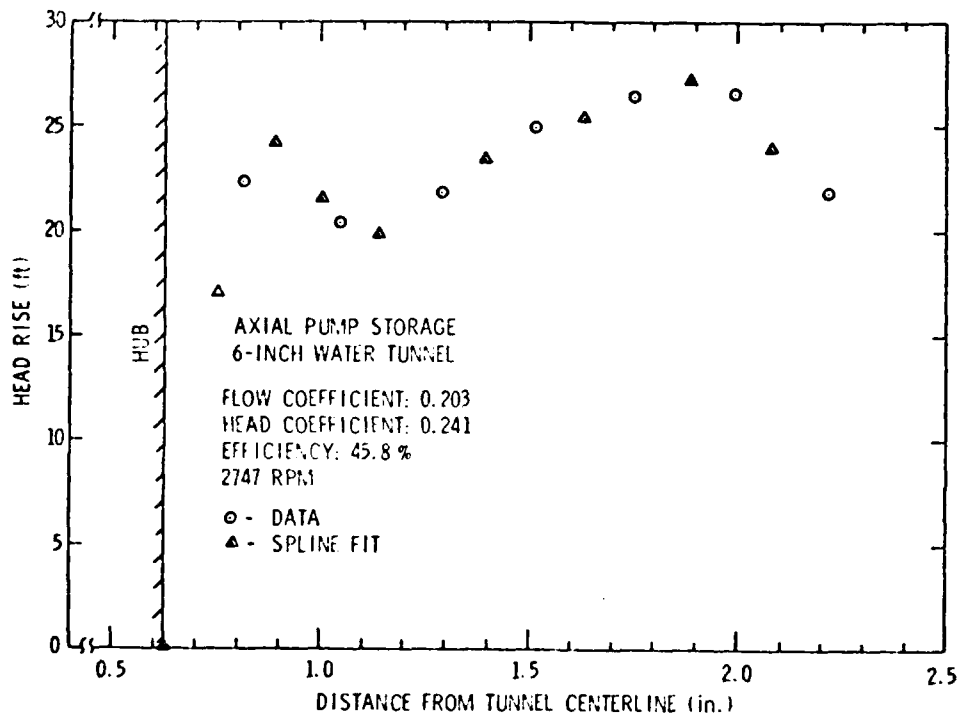


Figure 6: Pump Loading for Flow Coefficient of 0.203, 2747 RPM, and in Water

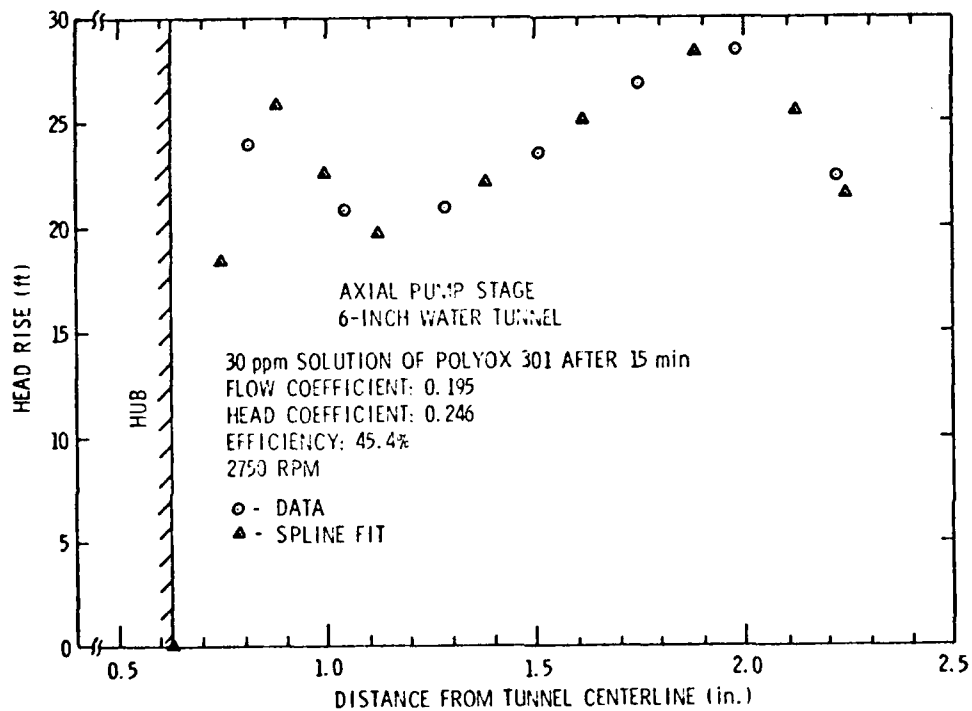


Figure 7: Pump Loading for Flow Coefficient of 0.195, 2750 RPM, and in 30 ppm Polymer Solution

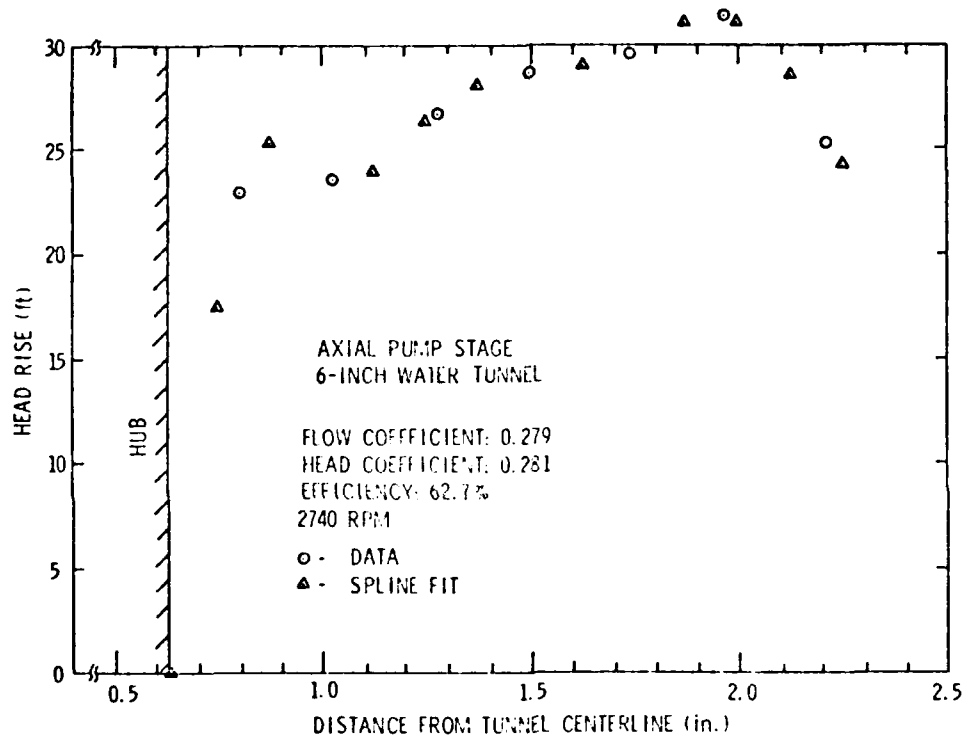


Figure 8; Pump Loading for Flow Coefficient of 0.279,  
2740 RPM, and in Water

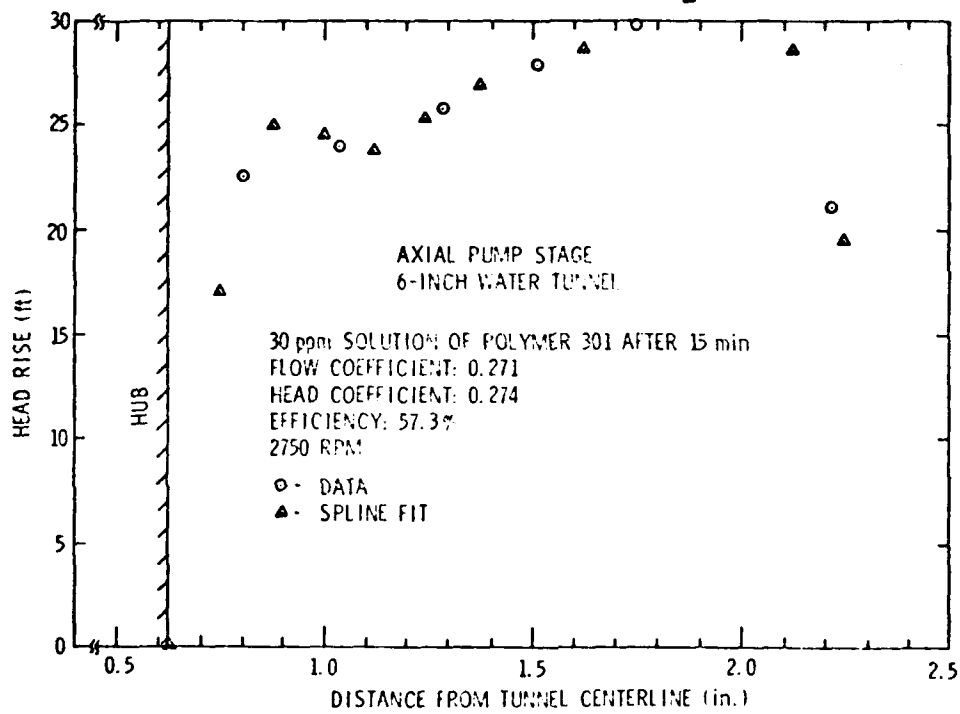


Figure 9: Pump Loading for Flow Coefficient of 0.271,  
2750 RPM, and in 30 ppm Polymer Solution

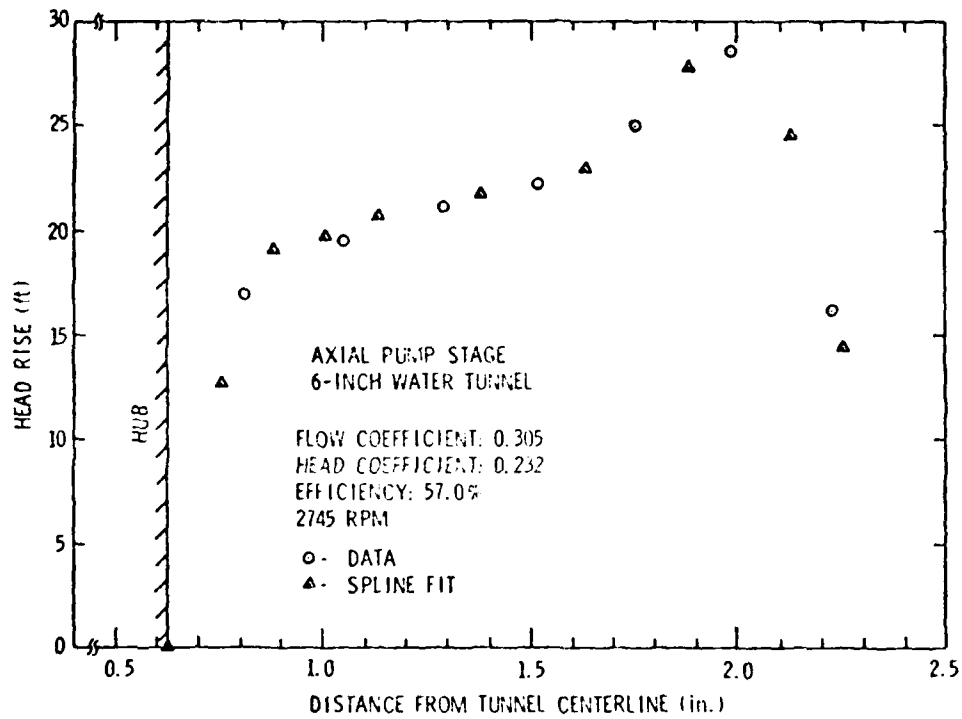


Figure 10: Pump Loading for Flow Coefficient of 0.305, 2745 RPM, and in Water



20 March 1975  
MLB:WSG:1hm

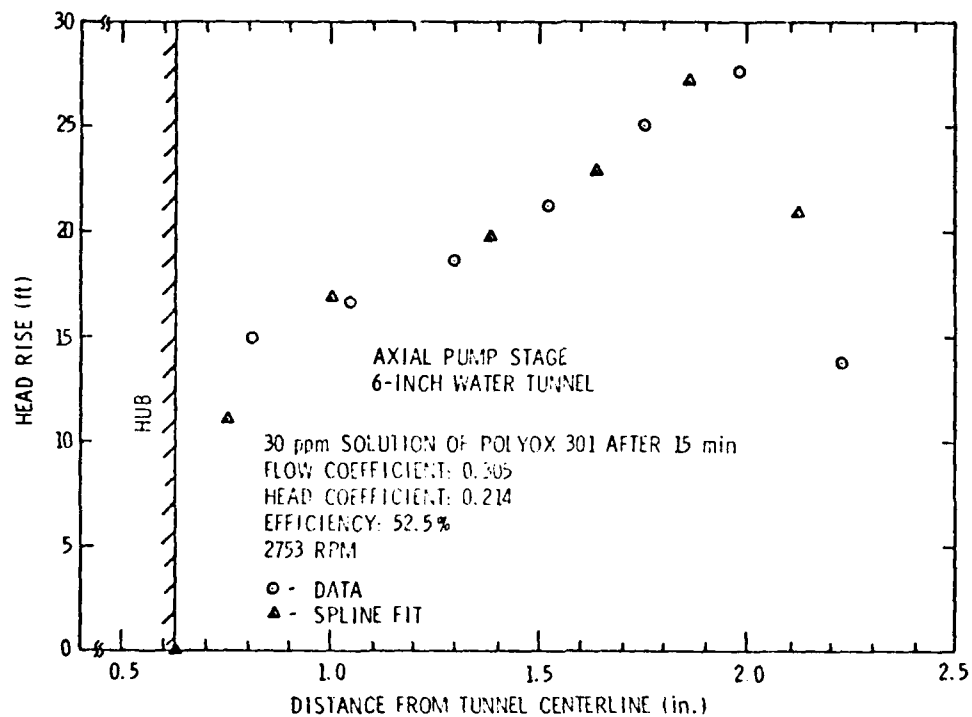


Figure 11: Pump Loading for Flow Coefficient of 0.305, 2753 RPM, and in 30 ppm Polymer Solution

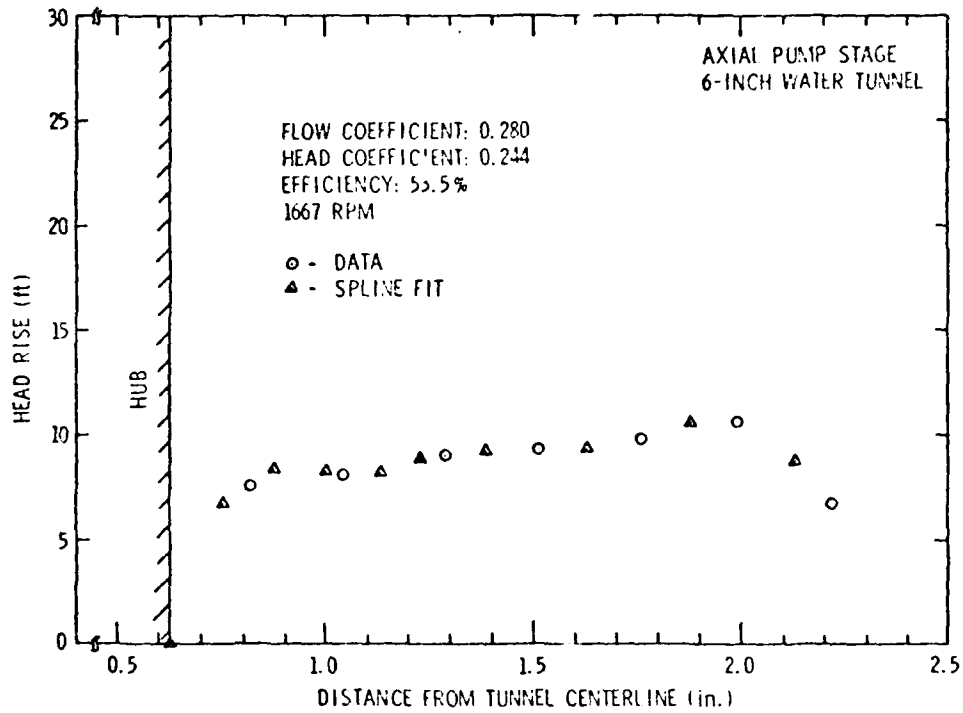


Figure 12: Pump Loading for Flow Coefficient of 0.280, 1667 RPM, and in Water

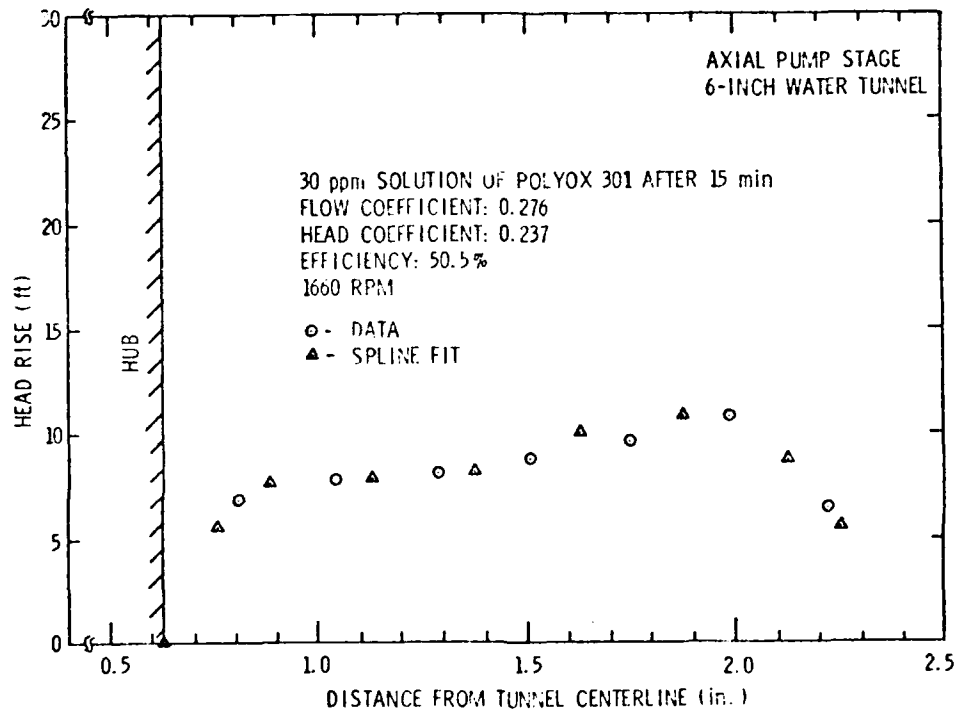


Figure 13: Pump Loading for Flow Coefficient of 0.276, 1660 RPM, and in 30 ppm Polymer Solution

20 March 1975  
MLB:WSG:1hm

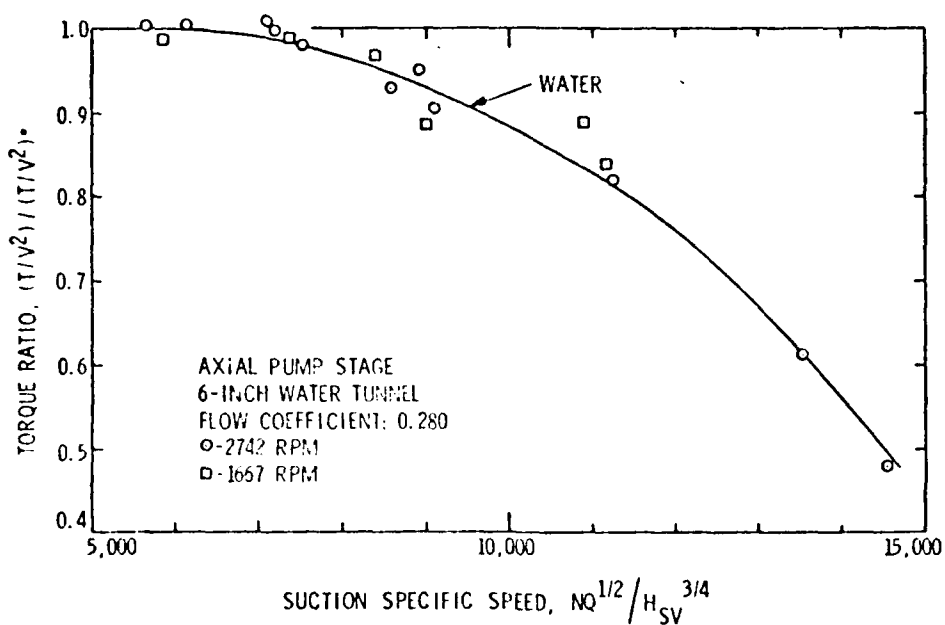


Figure 14: Pump Performance as a Function of Torque and Suction Specific Speed for a Flow Coefficient of 0.280 in Water

20 March 1975  
MLB:WSG:1hm

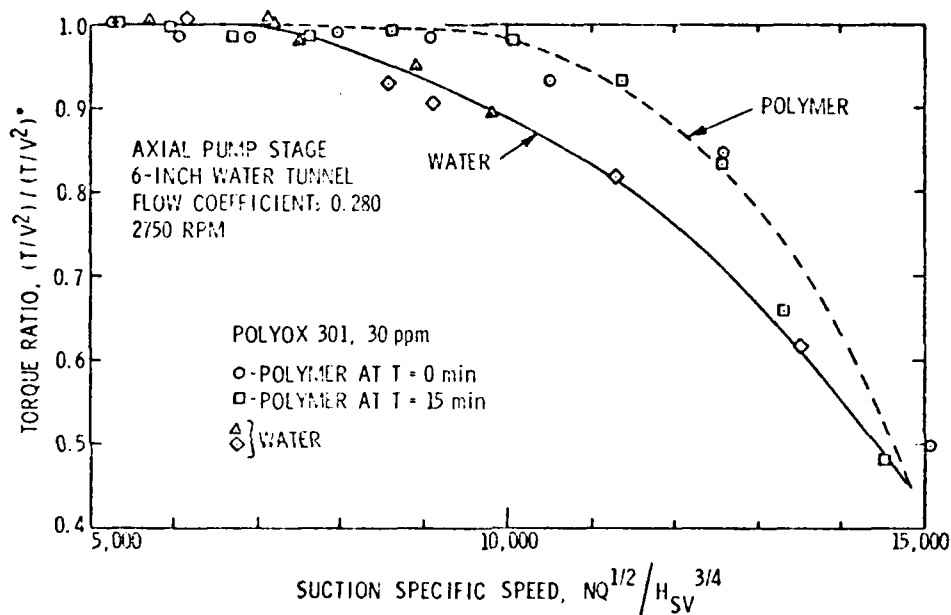


Figure 15: Pump Performance as a Function of Torque and Suction Specific Speed Operating in Water and Polymer Solution at a Flow Coefficient of 0.280 at 2750 RPM

20 March 1975  
MLB:WSG:1hm

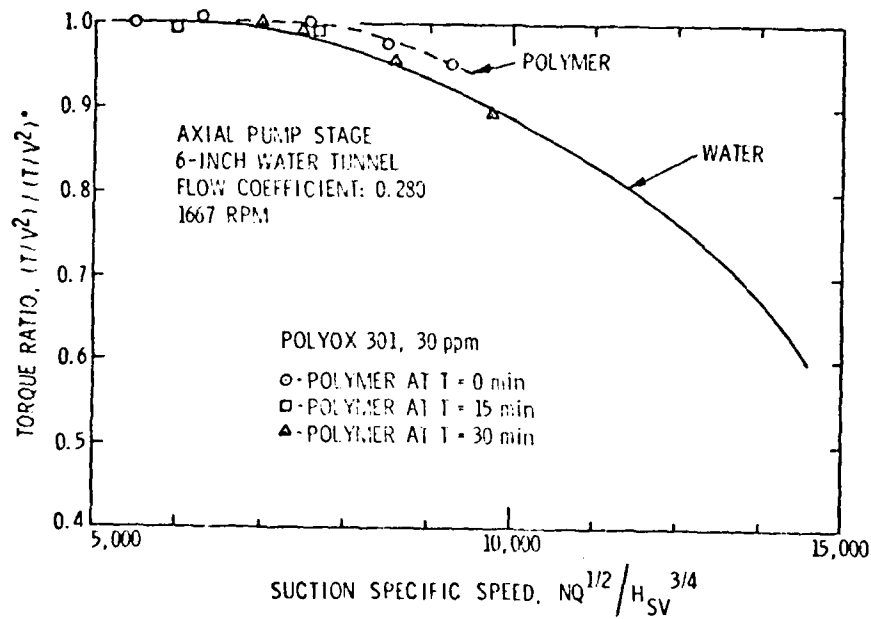


Figure 16: Pump Performance as a Function of Torque and Suction Specific Speed Operating in Water and Polymer Solution at a Flow Coefficient of 0.280 at 1667 RPM

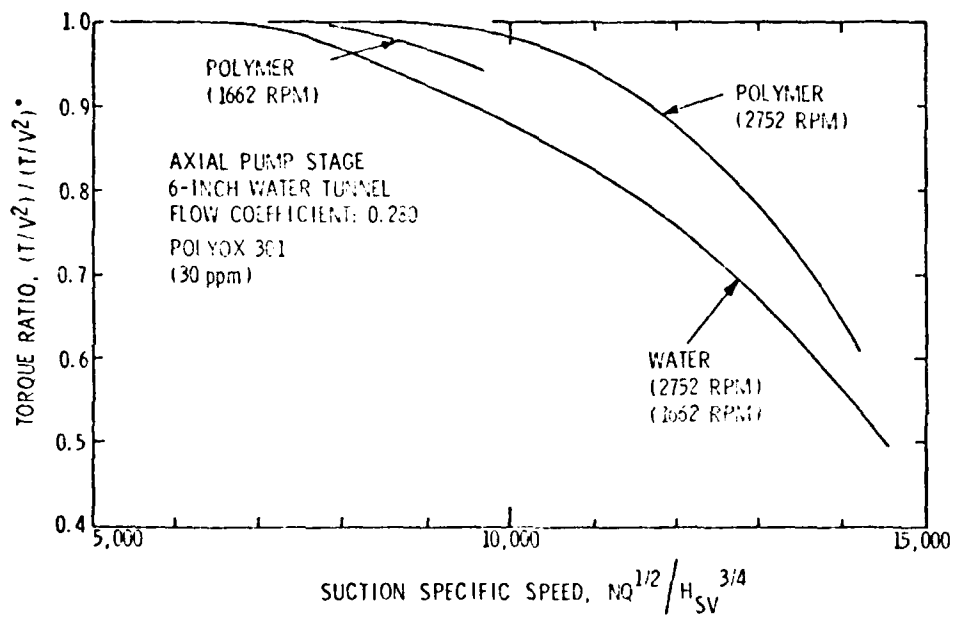


Figure 17: Summary of Pump Performance at a Flow Coefficient of 0.280 and both 2752 and 1662 RPM

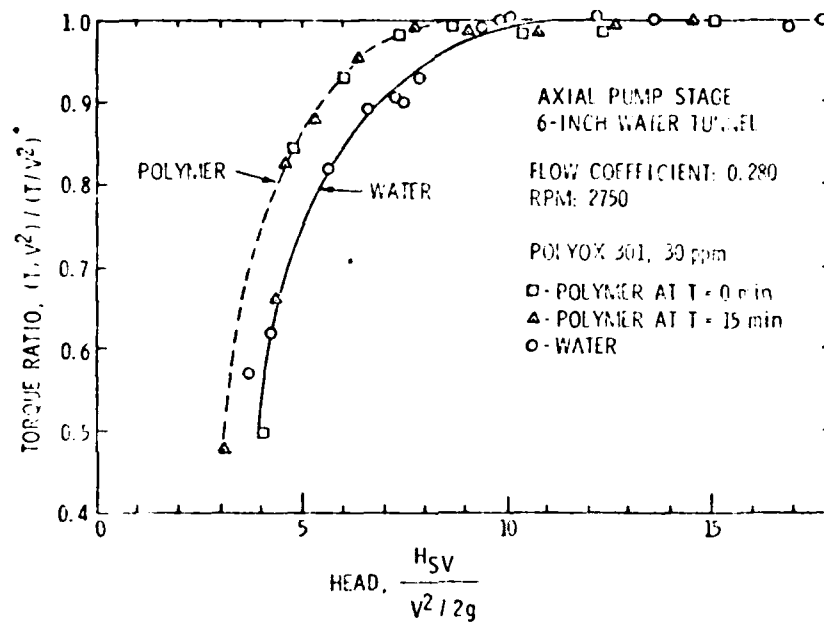


Figure 18: Pump Performance as a Function of Torque and Head Operating in Water and Polymer Solution at a Flow Coefficient of 0.280 at 1667 RPM



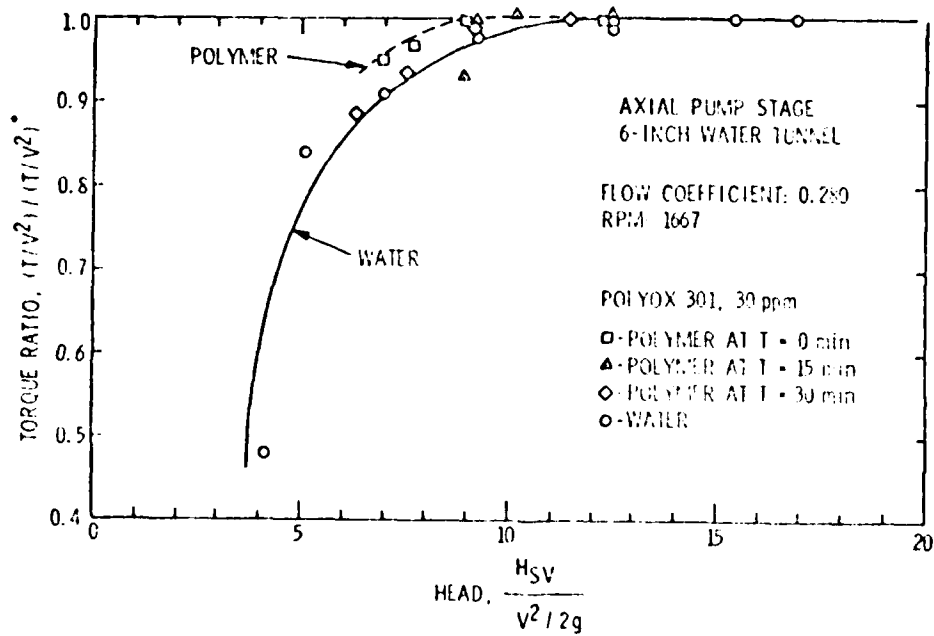


Figure 19: Pump Performance as a Function of Torque and Head Operating in Water and Polymer Solution at a Flow Coefficient of 0.280 at 1667 RPM

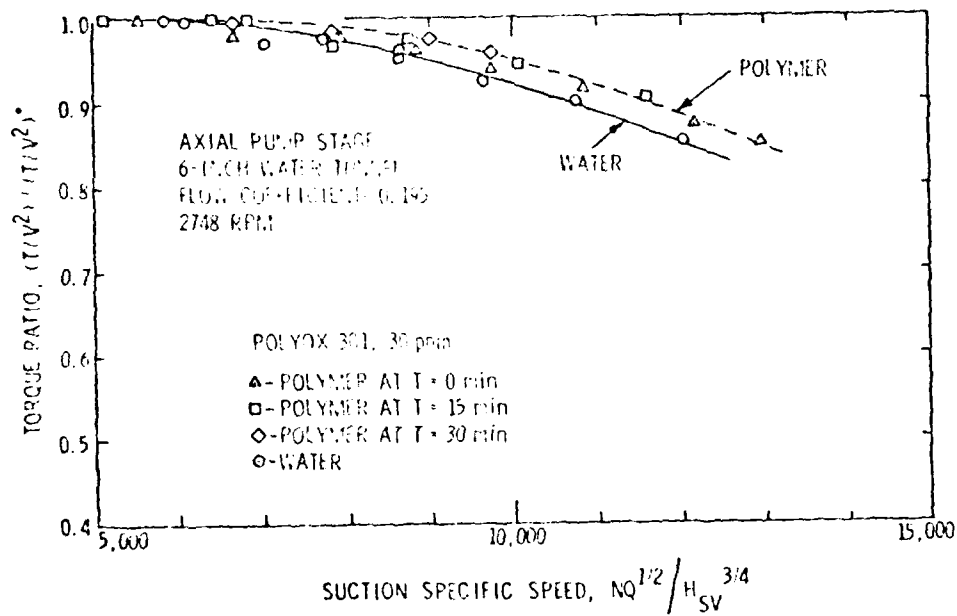


Figure 20: Pump Performance as a Function of Torque and Suction Specific Speed Operating in Water and Polymer Solution at a Flow Coefficient of 0.195 at 2748 RPM

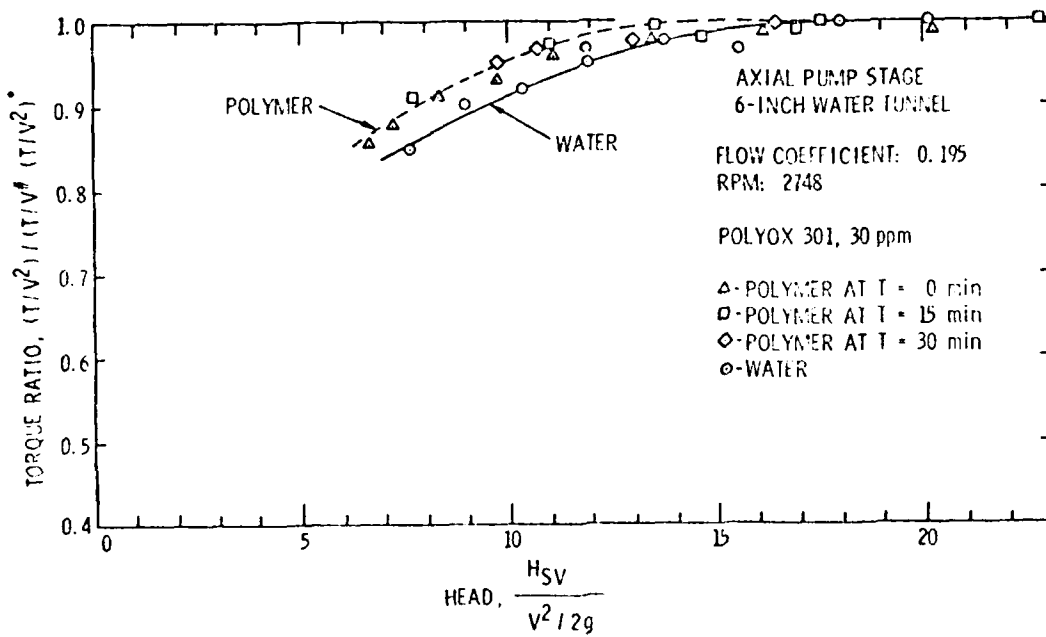


Figure 21: Pump Performance as a Function of Torque and Head Operating in Water and Polymer Solution at a Flow Coefficient of 0.195 at 2748 RPM

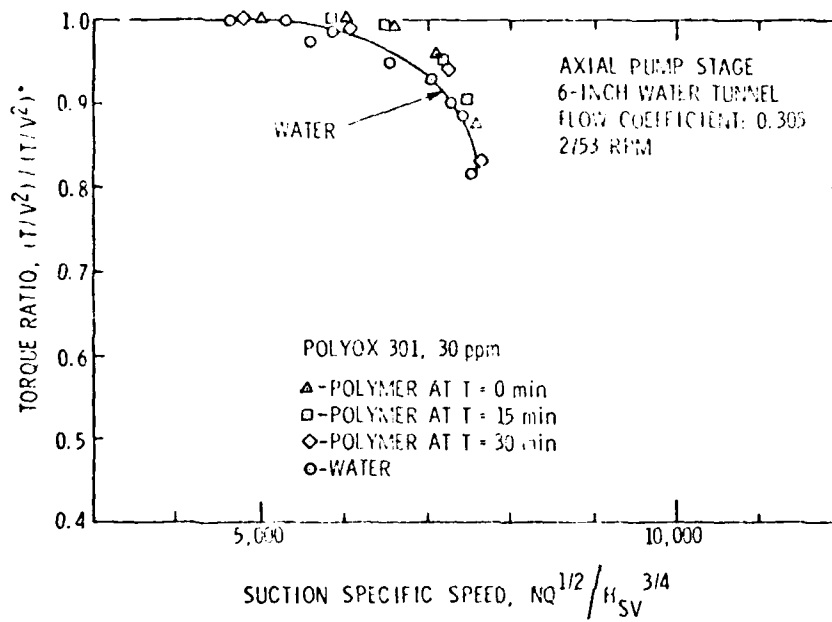


Figure 22: Pump Performance as a Function of Torque and Suction Specific Speed Operating in Water and Polymer Solution at a Flow Coefficient of 0.305 at 2753 RPM

20 March 1975  
MLB:WSG:1hm

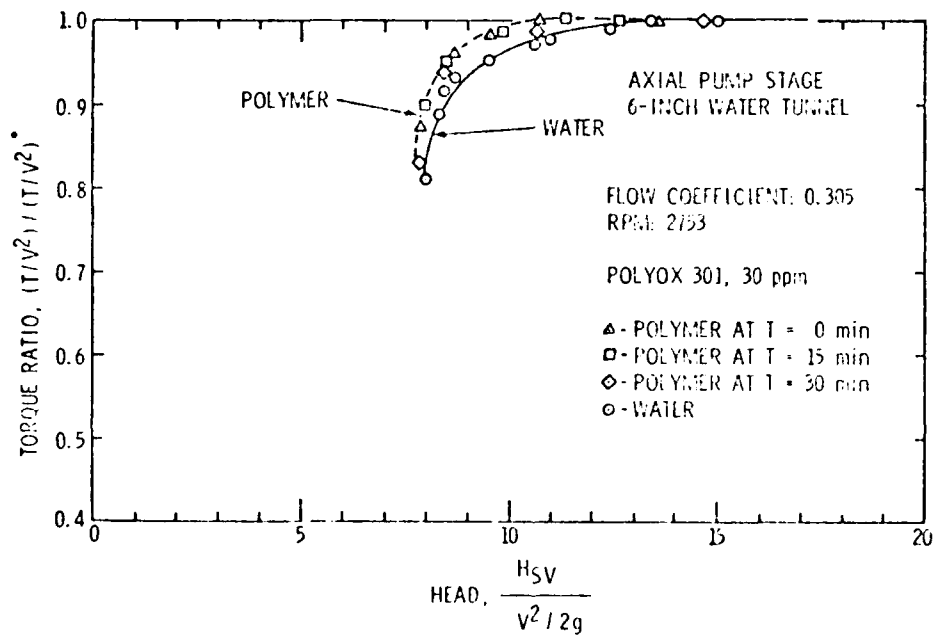


Figure 23: Pump Performance as a Function of Torque and Head Operating in Water and Polymer Solution at a Flow Coefficient of 0.305 at 2753 RPM

20 March 1975  
MLB:WSG:1hm

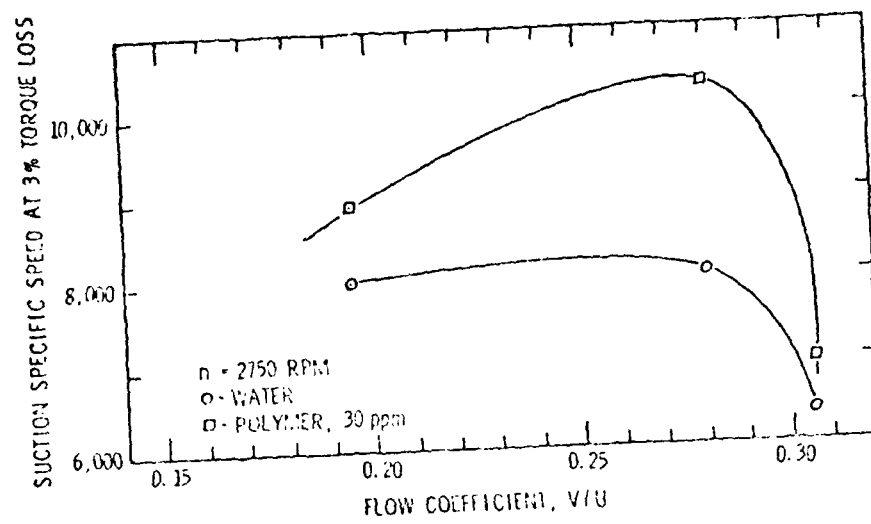


Figure 24: Summary of Polymer Influence on Pump Performance

20 March 1975  
MLB:WSG:1hm

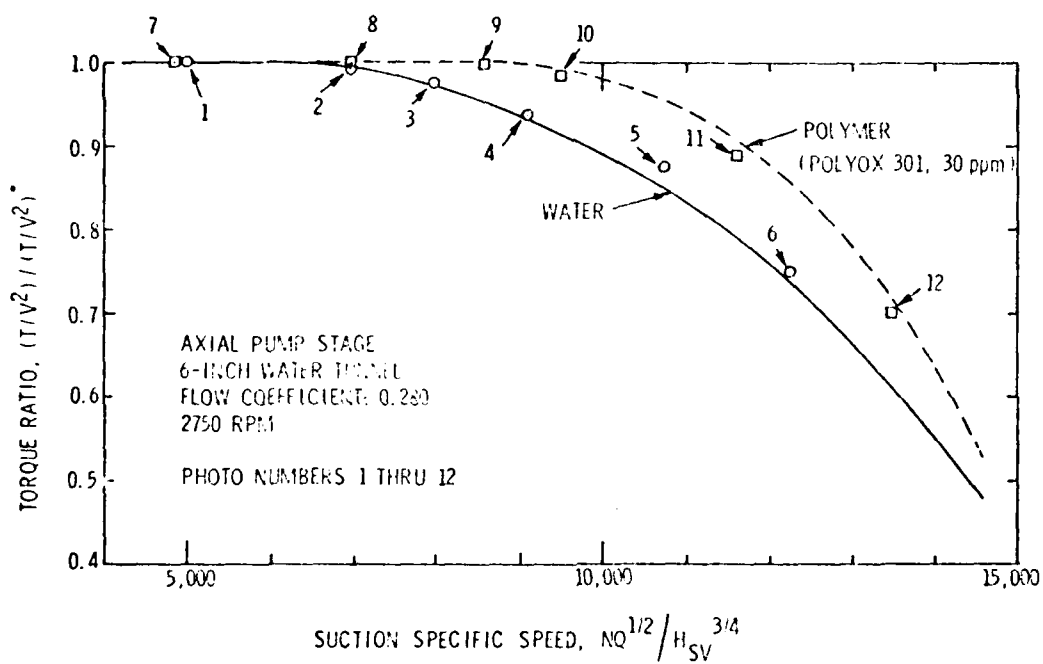


Figure 25: Index for Photographs of Pump Operating in Water and Polymer Solution at a Flow Coefficient of 0.280 at 2750 RPM

20 March 1973  
MB:MSO:129

-17-

Photograph #7

Flow Coefficient = 0.230  
2750 RPM

Photograph #1



Figure 26: Photograph of cavitation pump operating in stable and Polymer Solution

Reproduced from  
best available copy.





Polymer Solution  
Photograph #8

Flow Coefficient = 0.280  
2750 RPM

Photograph #2

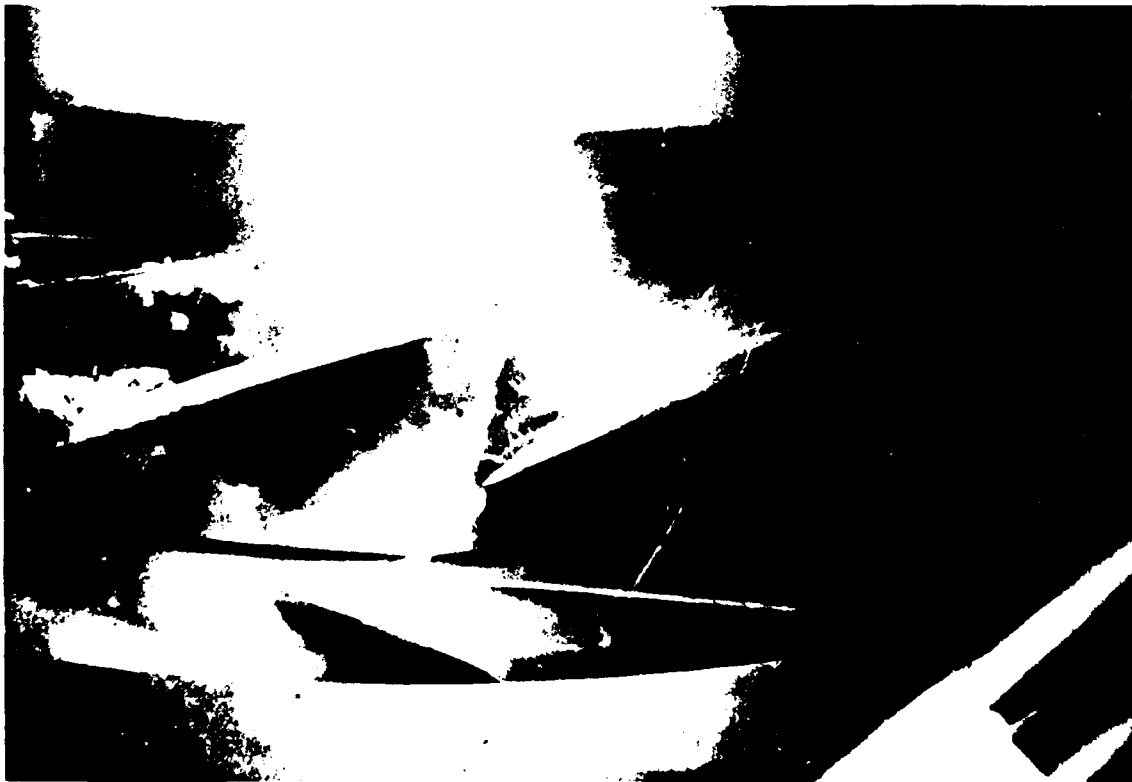
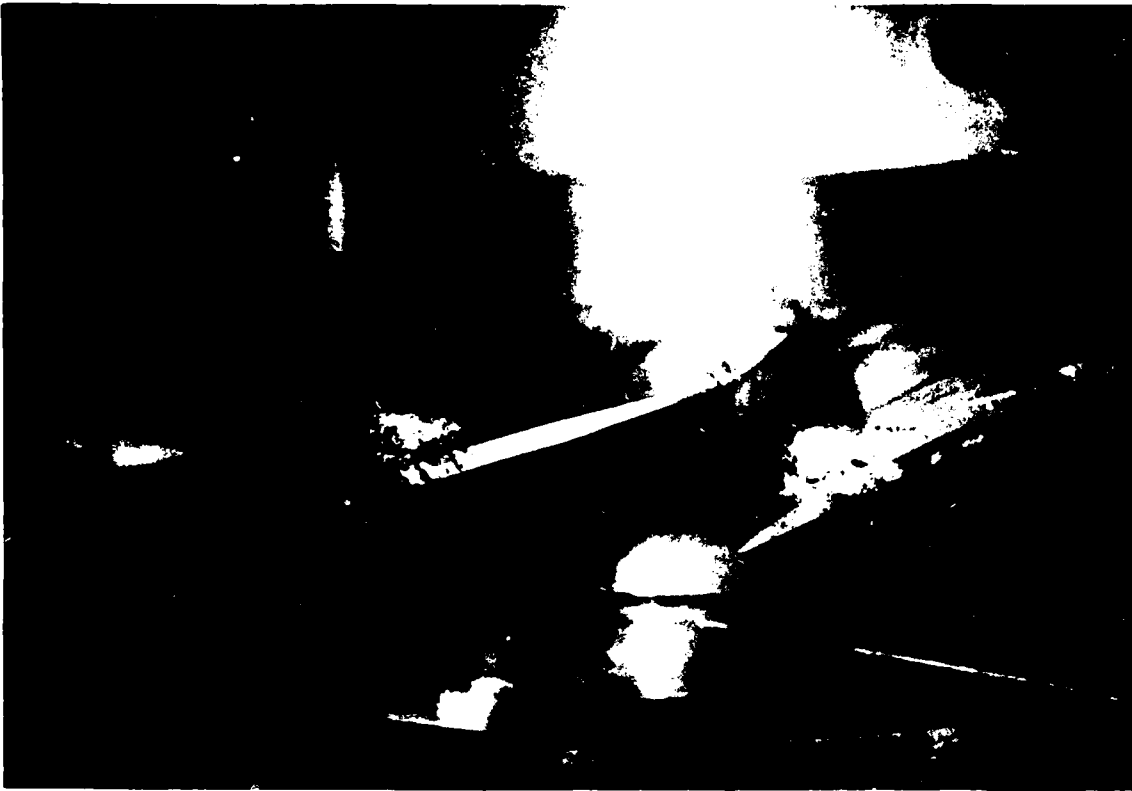
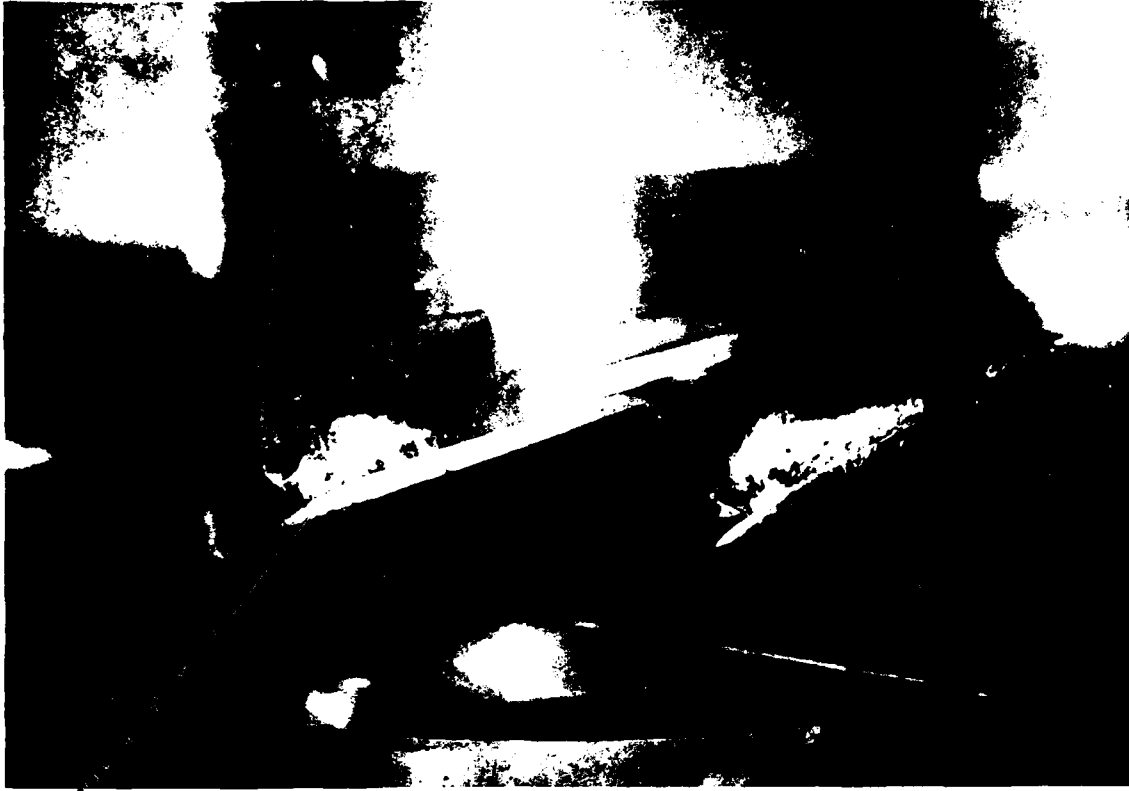


Figure 26: Photograph of Cavitating Pump Operating in Water and Polymer Solution



Polymer Solution  
Photograph #9



Flow Coefficient - 0.280  
2750 RPM

Water  
Photograph #3



Figure 26: Photograph of Cavitating Pump operating in Water and Polymer Solution



20 March 1975  
MLB:WSG:1hm

-40-

Polymer Solution  
Photograph #10



Flow Coefficient - 0.280  
2750 RPM

Water  
Photograph #4



Reproduced from  
best available copy.



Figure 26: Photograph of Cavitating Pump Operating in Water and Polymer Solution

20 March 1975  
MLB:WSG:1hm

-41-

Polymer Solution  
Photograph #11

Flow Coefficient - 0.280  
2750 RPM

Water  
Photograph #5



Figure 26: Photograph of Cavitating Pump Operating in Water and Polymer Solution

Reproduced from  
best available copy.



20 March 1975  
MLB:WSG:1hm

-42-

Polymer Solution  
Photograph #12



Water  
Photograph #6  
2750 RPM



Figure 26: Photograph of Cavitating Pump Operating in Water and Polymer Solution

Reproduced from  
best available copy.

